Development 126, 5749-5758 (1999)
Printed in Great Britain © The Company of Biologists Limited 1999
DEV2491

Mouse Pitx2 deficiency leads to anomalies of the ventral body wall, heart, extra- and periocular mesoderm and right pulmonary isomerism

Kunio Kitamura[1,‡], Hirohito Miura[1,*], Sachiko Miyagawa-Tomita[2], Masako Yanazawa[1], Yuko Katoh-Fukui[1], Rika Suzuki[1], Hideyo Ohuchi[3], Atuko Suehiro[1], Yoshiko Motegi[1], Yoko Nakahara[1], Shunzo Kondo[1] and Minesuke Yokoyama[1]

[1]Mitsubishi Kasei Institute of Life Sciences, 11 Minamiooya, Machida, Tokyo 194-8511, Japan
[2]Department of Pediatric Cardiology, The Heart Institute of Japan, Tokyo Women's Medical University, 8-1 Kawada-cho, Shinjuku-ku, Tokyo 162-8666, Japan
[3]Department of Genetic Biochemistry, Faculty of Pharmaceutical Sciences, Kyoto University Graduate School of Pharmaceutical Sciences, Kyoto 606-8501, Japan
*Present address: National Food Research Institute, Ministry of Agriculture, Forestry and Fisheries, 2-1-2 Kannondai, Tsukuba, Ibaraki 305-8642, Japan
‡Author for correspondence (e-mail: kunio@libra.ls.m-kagaku.co.jp)

Accepted 6 October; published on WWW 24 November 1999

SUMMARY

Pitx2, a bicoid-related homeobox gene, is involved in Rieger's syndrome and the left-right (L-R) asymmetrical pattern formation in body plan. In order to define the genomic structure and roles of Pitx2, we analyzed the genomic structure and generated Pitx2-deficient mice with the *lacZ* gene in the homeobox-containing exon of *Pitx2*. We were able to show that among three isoforms of Pitx2, Pitx2c shows asymmetrical expression whereas Pitx2a, Pitx2b and Pitx2c show symmetrical expression. In *Pitx2*$^{-/-}$ embryos there was an increase in mesodermal cells in the distal end of the left lateral body wall and an amnion continuous with the lateral body wall thickened in its mesodermal layer. These changes resulted in a failure of ventral body wall closure. In lung and heart in which *Pitx2* is expressed asymmetrically, right pulmonary isomerism, atrioventricular canals with prominent swelling, and juxtaposition of the atrium were detected. The hearts failed to develop tricuspid and mitral valves and a common atrioventricular valve forms. Further, dysgenesis of the *Pitx2*$^{-/-}$ extraocular muscle and thickening of the mesothelial layer of cornea were observed in the ocular system where Pitx2 is expressed symmetrically, and these resulted in enophthalmos. The present study shows that Pitx2 expressed in various sites participates in morphogenesis through three types of actions: the involvement of asymmetric Pitx2 expression in the entire morphogenetic process of L-R asymmetric organs; the involvement of asymmetric Pitx2 expression in the regional morphogenesis of asymmetric organs; and finally the involvement of symmetric Pitx2 expression in the regional morphogenesis of symmetric organs.

Key words: Pitx2, Isoforms, Symmetric/asymmetric expression, Gene targeting, Rieger's syndrome, mouse

INTRODUCTION

Pitx2, a bicoid type homeobox gene, was first identified as the gene responsible for Rieger's syndrome (Semina et al., 1996). Rieger's syndrome, defined as a genetic disorder is an autosomal-dominant human disorder characterized by ocular anterior chamber anomalies causing glaucoma in more than 50% of those affected, dental hypoplasia, mild craniofacial dysmorphism and umbilical stump abnormalities (Rieger, 1935; Jorgensen et al., 1978). We also found that Pitx2 (our old name: Brx1) is a transcription factor expressed in the ventral diencephalon, zona limitans intrathalamica and midbrain (Kitamura et al., 1997). Recently, Pitx2 was reported to participate in the L-R asymmetrical pattern formation in body plan (Ryan et al, 1998; Yoshioka et al., 1998; Logan et al., 1998; Piedra et al., 1998; St. Amand et al., 1998). Pitx2 is expressed on the left side of the axis shortly after nodal is detected in the lateral plate mesoderm. The Pitx2 expression domain is larger than that of nodal, persists longer, and includes not only the left lateral plate mesoderm but also the left side of the developing gut and heart. Both nodal and lefty-2 can induce ectopic Pitx2 in chick embryos. If the right side of the axis of chick embryos is infected with retroviruses expressing Pitx2, both the heart and derivatives of the gut become left isomerized. Pitx2 is repressed in FGF8-deficient mice, while Shh-deficient mice show expression of Pitx2 in the bilateral mesoderm (Meyers and Martin, 1999). Hence, Pitx2 seems to act as a global executor of L-R patterns downstream of the genetic cascade that regulates asymmetry.

Pitx2 has three isoforms, although it is not yet known which of the isoforms are expressed symmetrically and which asymmetrically (Kitamura et al., 1997; Gage and Camper, 1997). We tried to determine the genomic structure of the *Pitx2* gene and then to characterize the expression pattern of each

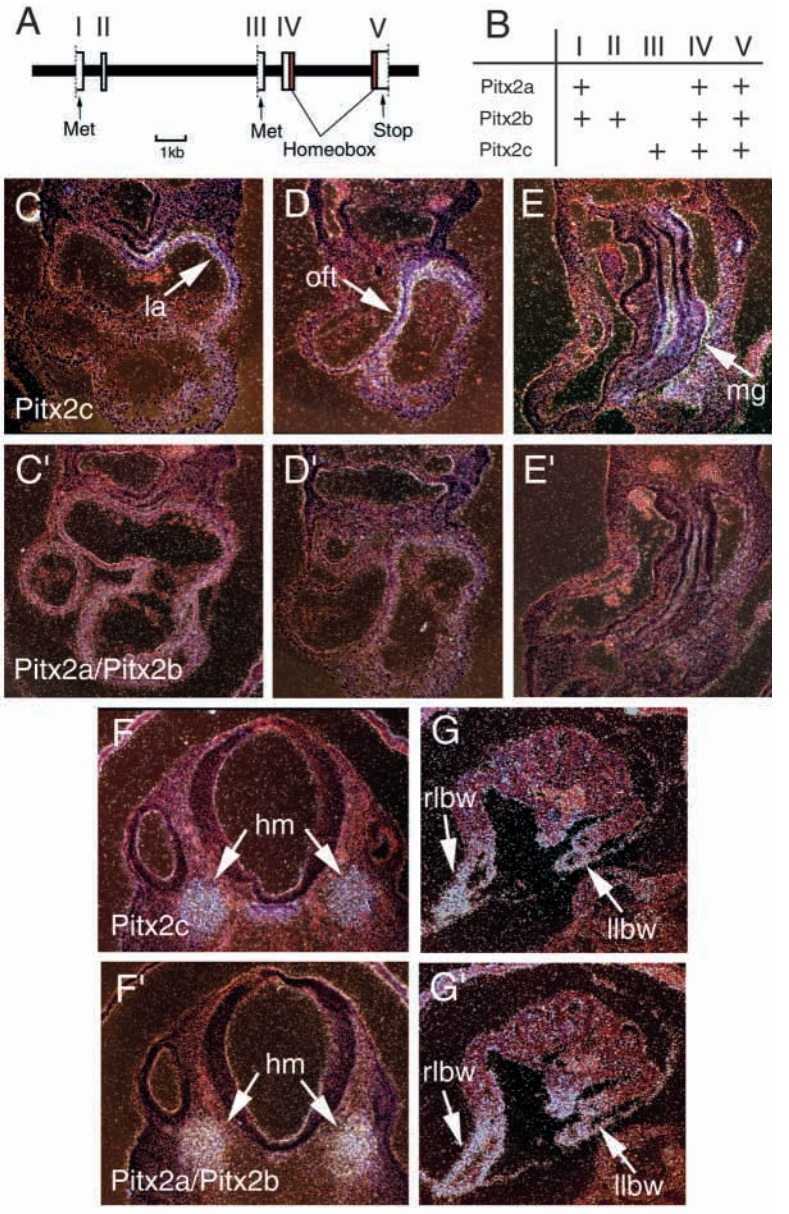

Fig. 1. Genomic structure of mouse *Pitx2* and expression patterns of three Pitx2 isoforms. (A) The *Pitx2* locus has at least 5 exons that code an open reading frame region of the three Pitx2 isoforms. (B) Assignment of each exon into three Pitx2 isoforms. Exon I is specific to Pitx2a and Pitx2b, exon II to Pitx2b, exon III to Pitx2c. Exons IV and V are common to all Pitx2 isoforms. (C-G, C′-G′) Expression of Pitx2c (C-G) and Pitx2a/Pitx2b (C′-G′) in ICR mouse embryos at 9.5 dpc. Specific probes for Pitx2c and Pitx2a/Pitx2b were prepared from cDNAs equivalent to exon III and exon I/exon II, respectively. Pitx2c is expressed in left atrium (la in C), left side of outflow tract (oft in D) and left side of midgut (mg in E), while very weak or no expression of Pitx2a/Pitx2b is seen in these organs (C′-E′). Symmetrical expression of both Pitx2c and Pitx2a/Pitx2b in head mesoderm (hm in F,F′) and the distal ends of the left and right lateral body wall (rlbw and llbw in G,G′).

isoform. Further, we generated Pitx2-deficient mice by homologous recombination in order to elucidate the in vivo function of Pitx2 in various expression sites. Homozygous *Pitx2*$^{-/-}$ embryos fail to close the ventral body wall and show cardiac malformation, anomalies of extra- and periocular mesoderm and right pulmonary isomerism, and finally die around days 14-15.

MATERIALS AND METHODS

Construction of the targeting vector

The *Pitx2* gene was cloned from a 129SVj mouse genomic library (Stratagene) using Pitx2 cDNA as a probe (Kitamura et al., 1997). The 4 independent genomic clones were isolated and the exon/intron structure was confirmed by sequence analysis (Fig. 1A). The reporter gene cassette '*IRES-T-lacZ*' derived from TV2 vector was used to construct the targeting vector (Takeuchi et al, 1995). The stop codon leading to termination of translation of *Pitx2* was inserted in front of IRES. The STOP-*IRES-T-lacZ* cassette and a 3 kb *Nru*I-*Sal*I fragment located at the 3′-position of the *Nru*I site in a homeobox and an *Eco*RI-*Xho*I fragment of pKJ2 were ligated and subcloned into pBluescript II (Fig. 2A; Boer et al., 1990). Further a 2.6 kb *Hin*dII-*Nru*I fragment located at the 5′-position of the *Nru*I site in the homeobox and the TK gene cassette were inserted in this order into the construct (Fig. 2A).

ES-cell transfection, screening and generation of *Pitx2*$^{-/-}$ mice

In order to obtain the targeted ES cells, we used a positive-negative selection strategy in the 129/Sv derived ES-cell line E14TG2a. The ES colonies were screened by Southern blot analysis with a 5′ and a 3′ probe external to the genomic sequences that were contained in the targeting vector and a Neo (Fig. 2A,B). Thirteen ES clones from 168 clones were found to have undergone homologous recombination (Fig. 2B).

The positive ES clones were injected into C57BL blastocysts and transferred into pseudopregnant female recipients. The resulting chimeric mice were bred with C57BL females. Transmission of the targeted *Pitx2* locus was confirmed from the Southern blot analysis. *Pitx2*$^{-/-}$ embryos used in the following analysis were obtained by crossbreeding F_2 *Pitx2*$^{+/-}$ mice (Fig. 2C). The *Pitx2*$^{-/-}$ homozygotes derived from the two independent targeted ES cell lines showed indistinguishable phenotypes.

In situ hybridization, X-gal staining and skeletal staining

Noon of the day after copulation was considered as day 0.5 p.c. In situ hybridization was performed as described previously (Kitamura et al., 1997). For X-gal staining, embryos were fixed with 0.2% glutaraldehyde/1% formalin/0.02% NP-40 for 2 hours, and if necessary, cryosections prepared from each embryo, and stained with X-gal. Skeletal preparation and staining was conducted essentially as described by Hogan et al. (1994).

Electron microscopy

Tissue for electron microscopy was fixed, stained and embedded using a conventional method. Thin sections were stained with uranyl-lead citrate before viewing in a JEOL 1200EX electron microscope.

RESULTS

Genomic structures of Pitx2a, Pitx2b and Pitx2c

We previously found two Pitx2 isoforms, Pitx2b (old name:

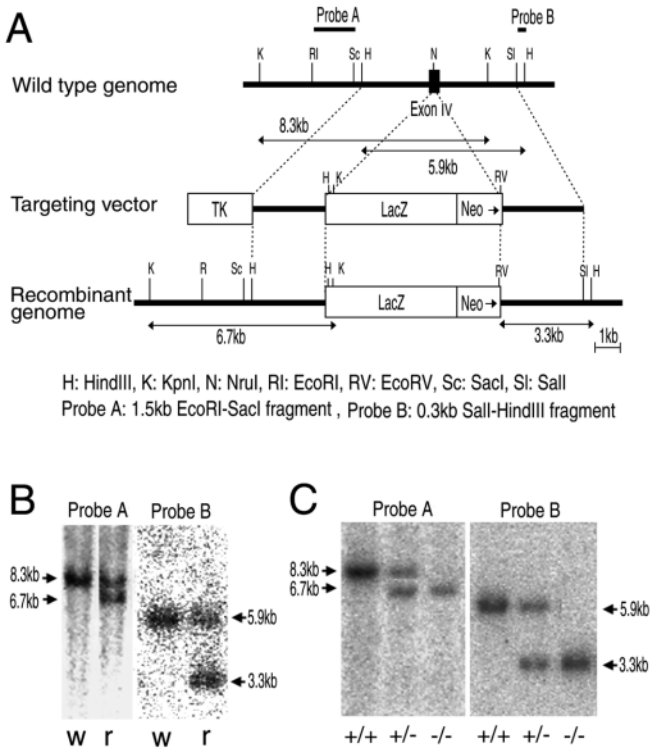

Fig. 2. Targeted disruption of the *Pitx2* gene. (A) Schematic representation of the wild type *Pitx2* gene locus (top), the targeting vector (middle) and the mutation-containing locus after homologous recombination (bottom). A STOP-*IRES*-*T*-*lacZ*-*Neo* cassette was inserted into *Nur*I site in exon IV. The orientation of the cassette is indicated by an arrow. (B) Southern blot analysis of targeted ES clones. Genomic DNA from cloned ES cells was digested with *Kpn*I and probed with probe A. Wild-type (w) and recombinant (r) loci generated 8.3 kb and 8.3 kb/6.7 kb fragments, respectively. Furthermore, the genomic DNA was digested with *Hin*dIII/*Eco*RV and probed with probe B. Wild-type and recombinant loci generated 5.9 kb and 5.9 kb/3.3 kb fragments, respectively. (C) Southern blot analysis of targeted yolk sac and embryos. Genomic DNA from a part of yolk sac or embryos at various stages were digested with *Kpn*I and probed with probe A. Wild-type (+/+) and homozygous (–/–) loci generated 8.3 kb and 6.7 kb fragments, respectively. Furthermore, the genomic DNA was digested with *Hin*dIII/*Eco*RV and probed with probe B. Wild-type (+/+) and homozygous (–/–) loci generated 5.9 kb and 3.3 kb fragments, respectively.

Brx1b, accession number: AB006321) and Pitx2c (old name: Brx1a, accession number: AB006320) from a mouse embryonic library (Kitamura et al., 1997). In the present study, we found another Pitx2 isoform, Pitx2a, which is the same as Rieg and otlx2 (Semina et al., 1996; Mucchielli et al., 1996; Gage and Camper, 1997). The structure of the *Pitx2* gene was examined in order to elucidate the exon/intron structure of the gene and assign each exon into one of the three isoforms. An open reading frame region of the three Pitx2 isoforms was found to consist of at least five exons (Fig. 1A). Exon I was specific to Pitx2a and Pitx2b, exon II only to Pitx2b, and exon III only to Pitx2c, and further exons IV and V were common to all Pitx2 isoforms (Fig. 1A). Thus, Pitx2a, Pitx2b and Pitx2c were alternative splicing products from one *Pitx2* gene. The human *RIEG* gene has a non-coding exon at the 5′-end, however, we were unable to find it in the present study (Semina et al., 1996).

Expression pattern of Pitx2a/Pitx2b and Pitx2c

We examined whether the complicated expression of Pitx2 could be regionally assigned to the expression pattern of each Pitx2 isoform. cDNA corresponding to exons I and II was too short to function as a specific probe for in situ hybridization of Pitx2a or Pitx2b, and therefore the expression of Pitx2a/Pitx2b and Pitx2c was examined in ICR mouse embryos at 9.5 dpc. Interestingly, asymmetric expression in the heart and gut was attributed to Pitx2c (Fig. 1C-E, compared with C′-E′), while

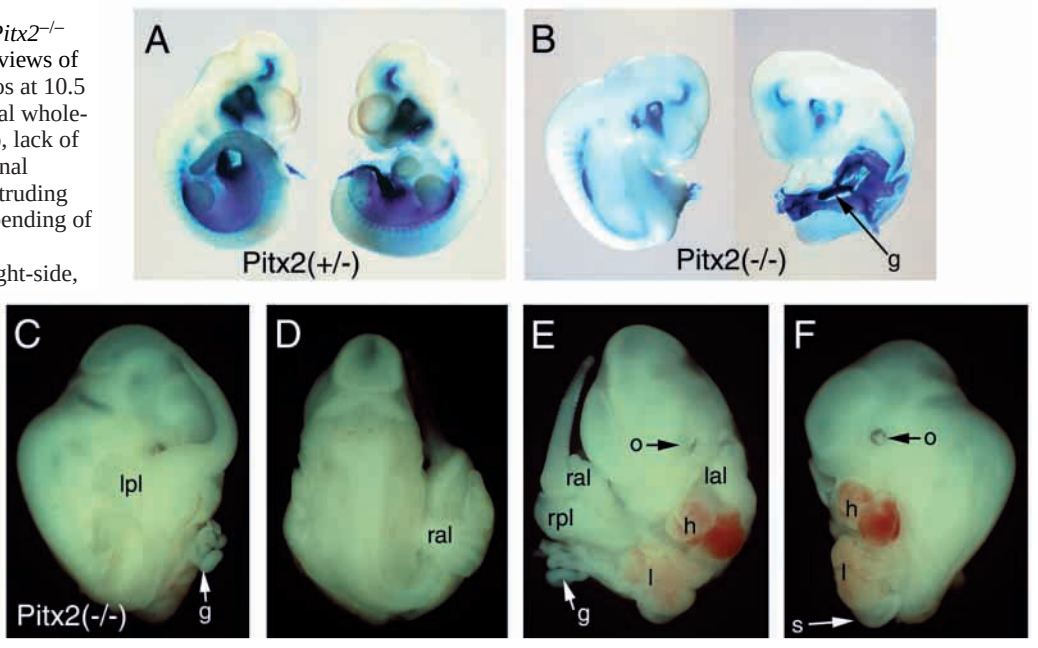

Fig. 3. Morphologic appearance of *Pitx2*$^{-/-}$ embryos. (A,B) Right- and left-side views of *Pitx2*$^{+/-}$ (A) and *Pitx2*$^{-/-}$ (B) embryos at 10.5 dpc. Embryos were treated with X-gal whole-mount staining. In a *Pitx2*$^{-/-}$ embryo, lack of ventral closure is seen in the abdominal region, and a part of the gut (g) is extruding toward the left side. Anticlockwise bending of the body axis is seen in the thoracic/abdominal region. (C-F) Right-side, dorsal, ventral and left-side views of *Pitx2*$^{-/-}$ embryos at 13.5 dpc, respectively. Extrusion of heart (h), liver (l), stomach (s) and gut (g) to the left side (E,F), anticlockwise bending of the body axis at the thoracic/abdominal region (C,D) and depression of the oculus (o) (E,F) are observed. lal, left anterior limb; lpl, left posterior limb; ral, right anterior limb; rpl, right posterior limb.

the symmetric expression in the head mesoderm and the lateral body wall was common to both the Pitx2a/Pitx2b and Pitx2c genes (Fig. 1F,F′,G,G′). Thus, only Pitx2c is expressed asymetrically.

Generation of *Pitx2*-deficient mice

To suppress the expression of all Pitx2 isoforms, we disrupted exon IV of the *Pitx2* gene by inserting the *lacZ* gene (Fig. 2A). The F_2 heterozygous crosses resulted in normal Mendelian ratios of homozygote, heterozygote and wild type (87:162:93) until 14.5 dpc, and thereafter no *Pitx2*$^{-/-}$ embryos were found. *Pitx2*$^{-/-}$ embryos at 10.5 dpc exhibited a lack of ventral closure (Fig. 3B, compared with A). Further, at 13.5 dpc, the typical morphology of *Pitx2*$^{-/-}$ embryos was extrusion of visceral organs (evisceration) to the left side, anticlockwise bending of the body axis at a thoracic/abdominal site and depression of the oculus (Fig. 3C-F). However, the morphology of the *Pitx2*$^{+/-}$ embryos was similar to that of the *Pitx2*$^{+/+}$ embryos.

Pitx2 deficiency results in failure of ventral body wall closure

Pitx2 is expressed in the left lateral plate mesoderm at 8-9 dpc and begins to be expressed in both the left and right distal ends of the lateral body wall mesoderm at 9.0-9.5 dpc (Fig. 4A,B). The right distal end extends towards the midline, while the left distal end extends towards the exterior at 9.0-9.5 dpc (Fig. 4C2). Along with development, the left distal end also comes close to the midline umbilical artery and ventral closure of the left and right body walls begins from the posterior end of the body axis (Fig. 4C1, F). In order to elucidate the differences in the orientation of the left distal ends of *Pitx2*$^{+/-}$ and *Pitx2*$^{-/-}$ embryos, we analyzed the number of *lacZ*(+) cells in the distal ends at 9.25-9.5 dpc. Cell counts were done in the two caudal regions, P-1 and P-2, because a change in the orientation of the left distal ends and the closure of both lateral walls are started from the caudal end of the body axis. The right distal ends in the P-1 and P-2 regions of both *Pitx2*$^{+/-}$ and *Pitx2*$^{-/-}$embryos extend internally (Fig. 4C1, C2, D1, D2), and the numbers of lacZ(+) cells of the right distal ends in the P-1 and P-2 region of *Pitx2*$^{-/-}$ embryos were each about 1.2 times those in *Pitx2*$^{+/-}$ embryos (Fig. 4E). The left distal ends in P-1 of *Pitx2*$^{+/-}$ embryos orient toward the axis, while those in *Pitx2*$^{-/-}$ embryos orient to the exterior (Fig. 4C1, D1). The number of lacZ(+) cells in the left P-1 of *Pitx2*$^{-/-}$ embryos was about 2.0 times that in *Pitx2*$^{+/-}$ embryos (Fig. 4E). Further, in the left P-2 region, although *Pitx2*$^{+/-}$ embryos have not yet finished changing the orientation of the distal end towards the axis (Fig. 4C2), the number of lacZ(+) cells in left distal end in P-2 of *Pitx2*$^{-/-}$ embryos was also about 1.8 to 1.9 times that in *Pitx2*$^{+/-}$ embryos (Fig. 4E).

A lot of *lacZ*(+) cells were found on the left half of the amnion ball of *Pitx2*$^{-/-}$ embryos (Fig. 4J, K, compared with H,I), and furthermore, the electron microscopic observations showed that the mesodermal cell layers of *Pitx2*$^{-/-}$ embryos are composed of 4 to 6 layers, while that of *Pitx2*$^{+/+}$ embryos was only one layer (Fig. 4M, compared with L). The increase in the number of lacZ(+) cells in the left distal end and the thickening of the lacZ(+) left amnion in the *Pitx2*$^{-/-}$ embryos are thought to result in a change of normal impetus, physical constraints and direction of the extending body wall. The left lateral body wall in *Pitx2*$^{-/-}$ embryos actually did not turn inwards, resulting in failure of the ventral body wall closure (Fig. 4G, compared with F).

Anticlockwise bending of the body axis was found at the thoracic/abdominal site in the *Pitx2*$^{-/-}$ embryos. In these embryos when the body wall failed to close there was extrusion of not only abdominal but also thoracic organs toward the left side (Fig. 3E,F). The left ribs splayed outwards, while the right ribs remained in the cartilage primordium of the proximal part of each rib and did not form the left part of the rib cage (* in Fig. 5B). The number of ribs was unchanged on both sides. In *Pitx2*$^{+/+}$/*Pitx2*$^{+/-}$ embryos at 11.0-11.5 dpc the loop of the midgut is formed in the abdominal cavity when the midgut extends and then rotates in an anticlockwise direction (–90°), but this primary rotation does not takes place in *Pitx2*$^{-/-}$ embryos (Fig. 5D, compared with C).

Pitx2 deficiency results in right pulmonary isomerism and complicated cardiac defects

In the wild type, Pitx2 was expressed only in the left bud of lung rudiment at 9.5 dpc (Fig. 5E,F). The right lung bud forms four lobes while the left lung bud only forms one. The asymmetric pattern of lung lobation was, however, altered in the *Pitx2*$^{-/-}$ embryos in which the left lung also had four lobes, in a mirror image to the right lung (Fig. 5H, compared with G). This condition is known as right pulmonary isomerism.

Development of the cardiovascular system in the *Pitx2*$^{-/-}$ embryos showed various patterning defects. At 10.5 dpc, the hearts of the *Pitx2*$^{-/-}$ embryos showed the same d-ventricular loop as normal hearts (Fig. 6A,B). However, the mutant hearts showed hypoplasia of the right ventricle and enlargement of the left atrium. It seemed that the mutant right ventricles were sometimes positioned on the left ventricle (not shown). In *Pitx2*$^{-/-}$ hearts at 11.5 dpc, a prominent swelling was seen at the atrioventricular (AV) canal region between the left atrium and left ventricle (arrowheads in Fig. 6D, compared with C). Inside the swelling of the *Pitx2*$^{-/-}$ heart, the AV cushions exhibited pronounced growth (Fig. 6E′). Expression of *lacZ* was seen in the prominent swelling at the AV canal region (Fig. 6D). In serial sections of *Pitx2*$^{-/-}$ embryos at 10.5 dpc, *lacZ* expression in the AV canal region was limited to the myocardium adjacent to the AV cushion but was not seen in the cushion tissues (arrows in Fig. 6F). *Pitx2*$^{-/-}$ hearts at 13.5 dpc failed to develop the tricuspid valve within the right ventricle and the mitral valve within the left ventricle, and formed a common AV valve on the left ventricle (arrows in Fig. 6H, compared with G). The right ventricle in the *Pitx2*$^{-/-}$ hearts was connected to the common AV valve through a ventricular septal defect (not shown).

The *Pitx2*$^{-/-}$ hearts had the morphological right atrial appendage juxtaposed with the morphological left atrial appendage at 13.5 dpc (Fig. 6J, compared with I. Arrowheads indicate left-sided juxtaposition of the atria). The atria of the *Pitx2*$^{-/-}$ hearts formed common atrium with an ostium primum atrial septal defect (not shown). In *Pitx2*$^{+/+}$/*Pitx2*$^{+/-}$ hearts at 13.5 dpc, both the left and right superior venae cavae and the inferior vena cava were connected to the right atrium, and the common pulmonary vein was connected to the left atrium (Fig. 6K,L). In contrast, the common atrium of the *Pitx2*$^{-/-}$ hearts was connected to the bilateral right and left superior venae

cavae, inferior vena cava, and common pulmonary vein (Fig. 6M,N).

The aorta is located posteriorly and to the right of the pulmonary trunk, and the aorta originates from the left ventricle and the pulmonary trunk from the right ventricle in *Pitx2*$^{+/+}$/*Pitx2*$^{+/-}$ hearts (Fig. 6G, I). In *Pitx2*$^{-/-}$ hearts, the aorta was located anteriorly and to the right of the pulmonary trunk, and both great arteries arose from the right ventricle (double outlet right ventricle) and were in parallel positions with the aorta located to the right of the pulmonary trunk (Fig. 6H,J).

Pitx2 deficiency results in extraocular muscle dysgenesis and thickening of the mesothelial layer of the cornea

Pitx2 is expressed in extraocular muscles, as shown by the coexpression of Pitx2 with myogenin and myf5 (Fig. 7A-C). In *Pitx2*$^{-/-}$ embryos, no expression of myogenin or myf5 was found at 12.5 dpc (Fig. 7D,E) and no extraocular muscle was formed, while Pitx2-expressing tongue muscles were formed normally (Fig. 7H,I). Further, it is noted that no *lacZ*(+) cells were detected in the extraocular muscle forming region (Fig. 7G, compared with arrowheads in F). Along with the deletion of extraocular muscles, in *Pitx2*$^{-/-}$ embryos there was a 5- to 10-fold increase in thickening of the *lacZ*(+) mesothelial layer of the cornea between cuboidal epithelium constituting the anterior part of the lens and cornea ectoderm at 12.5-13.5 dpc (Fig. 7G, compared with F; Kaufman, 1998). The thick mesothelial layer was invaded by the cuboidal epithelium of the anterior lens after 12.5 dpc (Fig. 7G). The extraocular muscle dysgenesis and corneal thickening resulted in enophthalmos.

DISCUSSION

Deficiency of FGF8, an upstream factor in the genetic cascade that participates in L-R asymmetry in the vertebrate body plan, results in asymmetrical abnormalities at the organ level in the lung, heart and digestive tube (Meyers and Martin, 1999). The present study has shown that Pitx2, a downstream factor, also participates in asymmetry of lung at the organ level (right pulmonary isomerism), while asymmetrical abnormalities of the heart and digestive tube at the organ level (reversed looping and situs) were not observed in the Pitx2 deficient embryos. However, the present results indicated that Pitx2 plays important roles in the various phases of asymmetric morphogenesis of heart and gut and symmetric morphogenesis of lateral body wall and extra- and periocular mesoderm. The latter anomalies in the morphogenesis are closely related to Rieger's syndrome.

Three isoforms of Pitx2

We have shown that three isoforms of Pitx2 are derived by an alternative splicing of the *Pitx2* gene, and that only Pitx2c is expressed asymmetrically. As Pitx2c is also expressed symmetrically in the head and lateral body wall, it is under dual control. Thus, it is expected that ectopic expression of upstream genes of *Pitx2* will result in the induction of Pitx2c in the right lateral plate mesoderm. Pitx2 has been ectopically expressed in chick embryos using Pitx2a (Logan et al., 1998). Nevertheless, the ectopic expression resulted in the asymmetrical effects on the morphology of the heart and gut. Thus, this shows that the asymmetrical effects of Pitx2 are carried by exons IV and V which are part of the homeobox and the 3′ region downstream to the homeobox.

Body wall and Pitx2

Pitx2 is expressed in the left lateral plate mesoderm of mouse and chick embryos (Ryan et al, 1998; Yoshioka et al., 1998; Logan et al., 1998; Piedra et al., 1998; Campione et al., 1999). Ectopic Pitx2 expression in chick embryos at stage 4 was shown to result in a reversal in the direction of embryonic rotation (Ryan et al., 1998), while in the present study, Pitx2-deficient mouse embryos showed no reversal of axial rotation at 8-9 dpc and thus were different from *situs inversus* (*iv/iv*) mutant embryos (Hummel and Chapman, 1959). Although the reason for this is unknown, the deficiency of Pitx2 may not result in the activation of cell proliferation in right lateral plate mesoderm and in right extraembryonic membrane at 8.0-9.0 dpc (Miller and White, 1998).

The effects of Pitx2 deficiency were first found in the left lateral body wall of the embryos at 9.25-9.5 dpc. An increase in the *Pitx2*$^{-/-}$ cells (*lacZ* positive) was followed by the exterior bending of the distal end of the wall and thickening of the amnion. *Pitx2*$^{-/-}$ and *Pitx2*$^{+/-}$ mesodermal cells in the distal end also spread throughout the lateral body wall as development progressed after 9.5 dpc. However, the thickening of the amnion was not observed in *Pitx2*$^{+/+}$/*Pitx2*$^{+/-}$ embryos. Thus, the thickening of the amnion associated with the early increase of *Pitx2*$^{-/-}$ mesodermal cells in the left distal end at 9.25-9.5 dpc is thought to be very important for the exterior bending of the left lateral body wall. We attempted to detect the changes in expression of genes that are expressed in the body wall (BMP1, BMP2, BMP4, Prx1, Prx2), however, no changes in expression were observed. This strongly suggests that the changes in the left lateral body wall are due to physical constraints. This is supported in the case of *iv/iv* mutant embryos in which asymmetrical cell proliferation in the embryonic body and extraembryonic membrane results in axial rotation (Miller and White, 1998). Lack of ventral closure has not been reported in mice deficient in genes related to asymmetry, such as *FGF8*, *Shh*, *lefty-1* and *ActRII*. Furthermore, not only asymmetrically expressed Pitx2c but also symmetrically expressed Pitx2a/Pitx2b are present in the lateral body wall after 9.25 dpc. Thus, Pitx2 that causes a failure of ventral closure is under another genetic cascade which is different from the FGF8-derived genetic cascade for asymmetry.

Left-right asymmetry in lung, cardiac looping and Pitx2

Lung anatomy is a good indicator of asymmetry. Mice mutant in Shh and lefty-1, which are midline signals, have left lung isomerism, while mice mutant in FGF8 and ActRIIB, which are left sided signals, have right lung isomerism (Chiang et al., 1996; Oh and Li, 1997; Meno et al., 1998; Meyers and Martin, 1999). Deficiency of Pitx2 also resulted in right pulmonary isomerism. Thus, Pitx2 is involved in lung asymmetry at the organ level. In early development of the lung, the right bud of the lung rudiment is larger than the left one, and FGF10 is expressed in the right bud earlier than in the left one (Bellusci

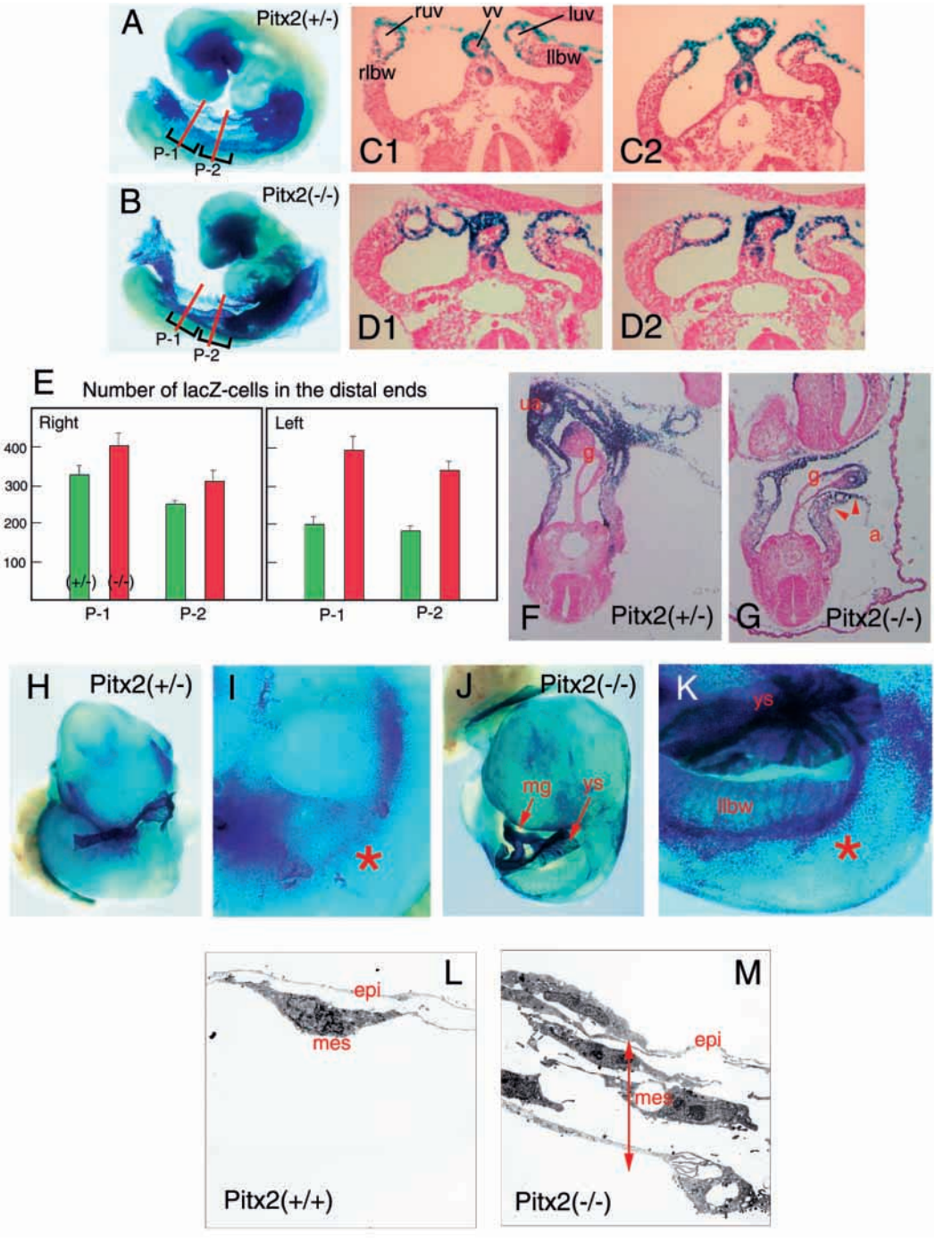

Fig. 4. Localization and numbers of *lacZ*-positive cells in the lateral body wall and electron microscopic images of amnion in *Pitx2*$^{-/-}$ embryos. (A,B) Left-side views of *Pitx2*$^{+/-}$ (A) and *Pitx2*$^{-/-}$ (B) embryos at 9.5 dpc. Morphological differences were not detected in either embryo. P-1 is the caudal region of the embryo and P-2 is the region that is anteriorly contiguous to P-1. P-1 and P-2 are each 400 μm in length. Red lines indicate approximate planes of sections (C1, C2, D1, D2). (C1, C2, D1, D2) X-Gal-stained serial sections from two regions, P-1 and P-2, of *Pitx2*$^{+/-}$ and *Pitx2*$^{-/-}$ embryos at 9.5 dpc. Distal ends of right lateral body wall (rlbw) of *Pitx2*$^{+/-}$ and *Pitx*$^{-/-}$ embryos turn inwards in both P-1 (C1, D1) and P-2 (C2, D2). Distal ends of left lateral body wall (llbw) of *Pitx2*$^{+/-}$ embryos turn inwards in P-1(C1) and outwards in P-2 (C2). However, distal ends of left lateral body wall of *Pitx2*$^{-/-}$ embryos turn outwards in both P-1 (D1) and P-2 (D2). luv, left umbilical vein; ruv, right umbilical vein; vv, vitelline vein. (E) Counts of *lacZ*-positive cells in the distal ends in P-1 and P-2 of *Pitx2*$^{+/-}$ and *Pitx2*$^{-/-}$ embryos at 9.5 dpc. For the cell counting, a *Pitx2*$^{+/-}$ and a *Pitx2*$^{-/-}$ embryo, each with the same somite number, were selected from one litter. Green bars show the number of *lacZ*-positive cells in Pitx2$^{+/-}$ embryos and red bars show the number of *lacZ*-positive cells in *Pitx2*$^{-/-}$ embryos. Each bar represents *lacZ*-positive cells in the extracted 10 sections from serial sections of each P-1 and P-2 region expressed as the cell number/5 sections. Counting was carried out for the three pairs of *Pitx2*$^{+/-}$ and *Pitx2*$^{-/-}$ embryos. Right (right distal ends): in P-1, the number of *lacZ*-positive cells in *Pitx2*$^{-/-}$ embryos was 1.2 times that in *Pitx2*$^{+/-}$ embryos. In P-2, the number of *lacZ*-positive cells in *Pitx2*$^{-/-}$ embryos was also 1.2 times that in *Pitx2*$^{+/-}$ embryos. Left (left distal ends): in P-1, the number of *lacZ*-positive cells in *Pitx2*$^{-/-}$ embryos was 2.0 times that in *Pitx2*$^{+/-}$ embryos. In P-2, the number of *lacZ*-positive cells in *Pitx2*$^{-/-}$ embryos was 1.8 to 1.9 times that in *Pitx2*$^{+/-}$ embryos. Bars show s.e.m. (F,G) X-gal stained sections from *Pitx2*$^{+/-}$ (F) and *Pitx2*$^{-/-}$ (G) embryos at 10.0 dpc. In *Pitx2*$^{+/-}$ embryos, the left and right lateral body walls close on the midline umbilical artery (ua). In *Pitx2*$^{-/-}$ embryos, the left lateral body wall bends outwards (red arrowheads in G) and thus the two lateral body walls are unable to close. a: amnion, g: gut. (H-K) Whole-mount X-Gal stained *Pitx2*$^{+/-}$ (H,I) and *Pitx2*$^{-/-}$ (J,K) embryos at 10.5 dpc. Embryos are covered with the amnion. In *Pitx2*$^{+/-}$ embryos, the amnion converges with the vitelline duct (H,I), while in *Pitx2*$^{-/-}$ embryos, the abdominal region is not covered by the amnion, and midgut (mg) connected to the vitelline duct/yolk sac (ys) is extruding (J), so that the vitelline duct cannot bind to the connecting stalk and fails to form a primitive umbilical cord. The amnion of *Pitx2*$^{-/-}$ embryos, which is contiguous with the lateral body wall (llbw), contains more *lacZ*-positive cells than those of *Pitx2*$^{+/-}$ embryos (* in K, compared with * in I). (L,M) Transmission electron microscopic images of amnions from *Pitx2*$^{+/+}$ (L) and *Pitx2*$^{-/-}$ (M) embryos at 10.5 dpc. In *Pitx2*$^{+/+}$ embryos, the amnion is composed of two single layers of epithelial cells (epi) and mesodermal cells (mes), while in *Pitx2*$^{-/-}$ embryos, the amnion is composed of a single layer of epithelial cells and 4 to 6 layers of mesodermal cells.

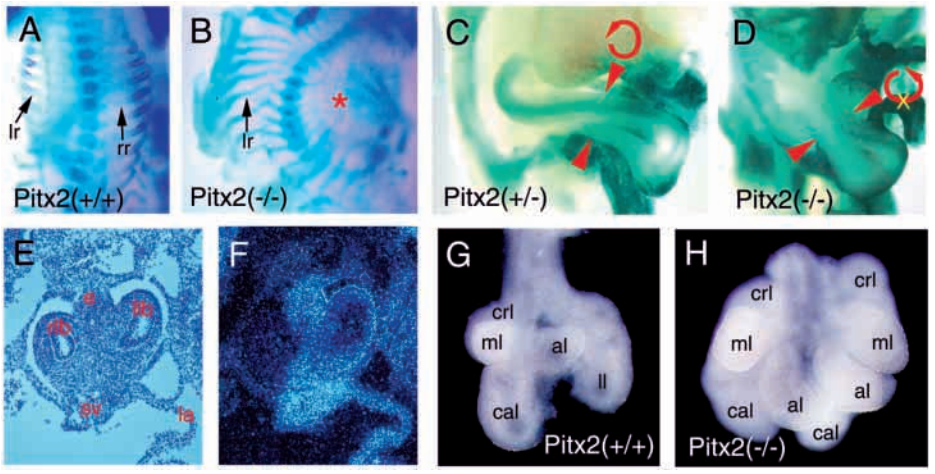

Fig. 5. Right rib dysgenesis, loss of primary midgut rotation and right pulmonary isomerism in *Pitx2*$^{-/-}$ embryos. (A,B) Dorsal views of skeleton of a *Pitx2*$^{+/+}$ (A) and *Pitx2*$^{-/-}$ (B) embryo at 13.5 dpc. In *Pitx2*$^{+/+}$ embryos, left (lr) and right (rr) rib cages are formed. In *Pitx2*$^{-/-}$ embryos, the left ribs splay outward, while the right ribs remain as the cartilage primordium in the proximal part of each rib and thus no left rib cage is formed (* in B). (C,D) Primary anticlockwise rotation of midgut is seen in a *Pitx2*$^{+/-}$ embryo at 11.5 dpc (red arrowheads in C), while the primary rotation does not occur in a *Pitx2*$^{-/-}$ embryo at 11.5 dpc (red arrowheads in D). (E,F) Bright-field image (E) and in situ hybridization image of Pitx2 (F) in lung bud of a wild-type embryo at 9.5 dpc. Pitx2 is not seen in the right lung bud (rlb) but in the left lung bud (llb), the left atrium (la) and left sinus venosus (sv) are Pitx2 positive. e, oesophagus. (G,H) In a *Pitx2*$^{+/+}$ embryo (G), the right lung has four lobes (crl, ml, cal, al) and the left lung has only one (ll), while the left lung also has four lobes in a *Pitx2*$^{-/-}$ embryo (H).

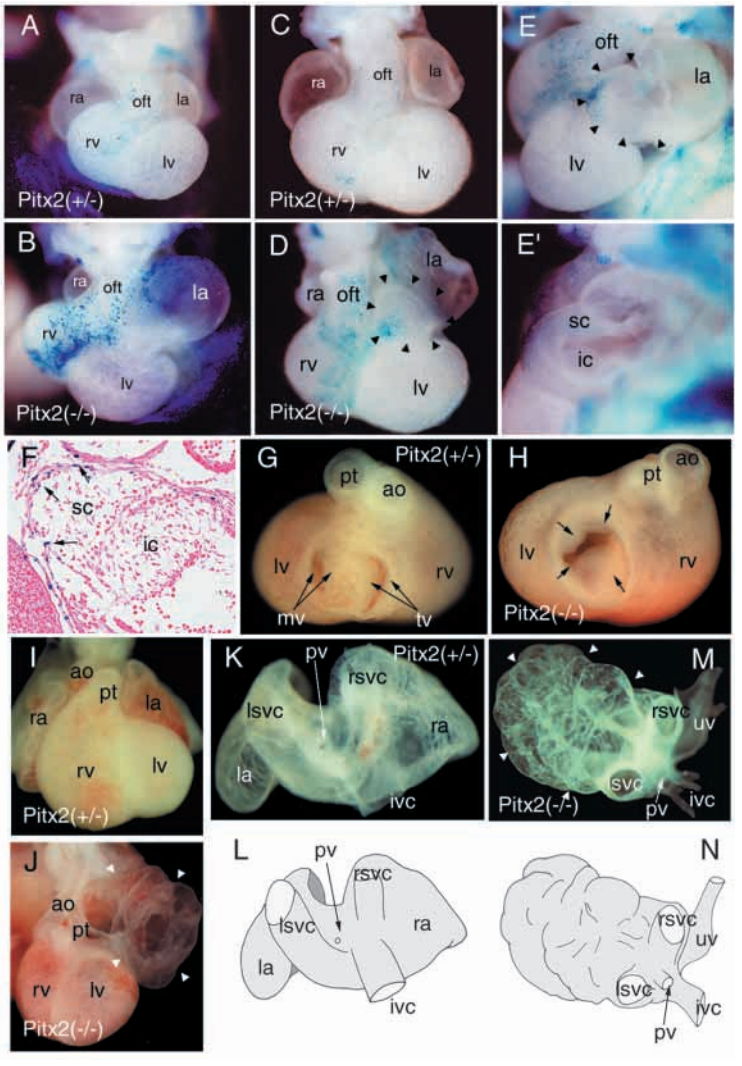

Fig. 6. Cardiovascular anomalies in *Pitx2*$^{-/-}$ embryos. *Pitx2*$^{+/-}$ (A,C,G,I,K,L) and *Pitx2*$^{-/-}$ (B,D-F,H,J,M,N) embryonic hearts. (A,C) Frontal view of *Pitx2*$^{+/-}$ hearts at 10.5 dpc (A) and 11.5 dpc (C). The right atrium (ra) is above the right ventricle (rv) and the left atrium (la) above the left ventricle (lv). The outflow tract (oft) is connected to the right ventricle. (B,D) Frontal view of the *Pitx2*$^{-/-}$ hearts at 10.5 dpc (B) and 11.5 dpc (D). The heart at 10.5 dpc shows the same d-ventricular loop as normal embryos but hypoplastic right ventricle and enlargement of the left atrium are seen. Distinctive expression of β-gal is observed in the left atrium, outflow tract, and the left side of the right ventricle. A prominent swelling (arrowheads in D) at the AV canal region between the left atrium and left ventricle is seen in the *Pitx2*$^{-/-}$ heart at 11.5 dpc. The right atrium shows an inadequate rightward shift. (E,E′) A prominent swelling (arrowheads in E) in the AV canal region at 11.75 dpc. (E) A part of the left atrium of a *Pitx2*$^{-/-}$ heart has been opened to allow viewing inside the swelling. (E′) Prominent growth of the superior AV cushion (sc) and inferior AV cushion (ic) is observed. (F) *Pitx2*$^{-/-}$ hearts at 10.5 dpc were serially sectioned. β-gal expression in the AV canal region is seen in the myocardium adjacent to the AV cushions (arrows), but not in the cushion tissues. Sc, superior cushion; ic, inferior cushion. (G,H) Most of the atrial and venous components of *Pitx2*$^{+/-}$ (G) and *Pitx2*$^{-/-}$ (H) mouse hearts at 13.5 dpc have been removed to allow viewing of the AV canal from above (cranially). In the *Pitx2*$^{+/-}$ mouse hearts, the tricuspid valve (tv) is formed within the right ventricle (rv) and the mitral valve (mv) within the left ventricle (lv). The aorta (ao) is located posteriorly and to the right of the pulmonary trunk (pt). In the *Pitx2*$^{-/-}$ mouse hearts, a common AV valve (arrows) can be seen. The common AV valve on the left ventricle is connected to the right ventricle through a ventricular septal defect (not shown). (I,J) Frontal view of *Pitx2*$^{+/-}$ (I) and *Pitx2*$^{-/-}$ (J) embryos at 13.5 dpc. The *Pitx2*$^{+/-}$ embryos show normal heart morphology. The aorta is located posteriorly and to the right of the pulmonary trunk. The aorta arises from the left ventricle and the pulmonary trunk from the right ventricle. The right atrium (ra) at the right side and left atrium (la) at the left side are connected to the right and left ventricles, respectively. In the *Pitx2*$^{-/-}$ embryos, the two great arteries are located in abnormal positions. The aorta is anterior and to the right of the pulmonary trunk (see also H). Both great arteries originate from the right ventricle. Left-sided juxtaposition of the atria (arrowheads) is seen. (K-N) Dorsal view of the atria at 13.5 dpc. L and N are drawings of the atria in K and M respectively. (K,L) In the *Pitx2*$^{+/-}$ mouse heart, the right atrium is connected to the right superior vena cava (rsvc) and inferior vena cava (ivc) through the venous valves. The left superior vena cava (lsvc), through the left horn of the sinus venosus along the posterior wall of the left atrium, is connected to the right atrium through the venous valves. The left atrium is connected to the common pulmonary vein (pv). (M,N) In the *Pitx2*$^{-/-}$ heart, a common atrium, showing left-sided juxtaposition of the atria (arrowheads), is connected to bilateral right and left superior venae cavae, the inferior vena cava, common pulmonary vein (arrow), and umbilical vein (uv) through the venous valves.

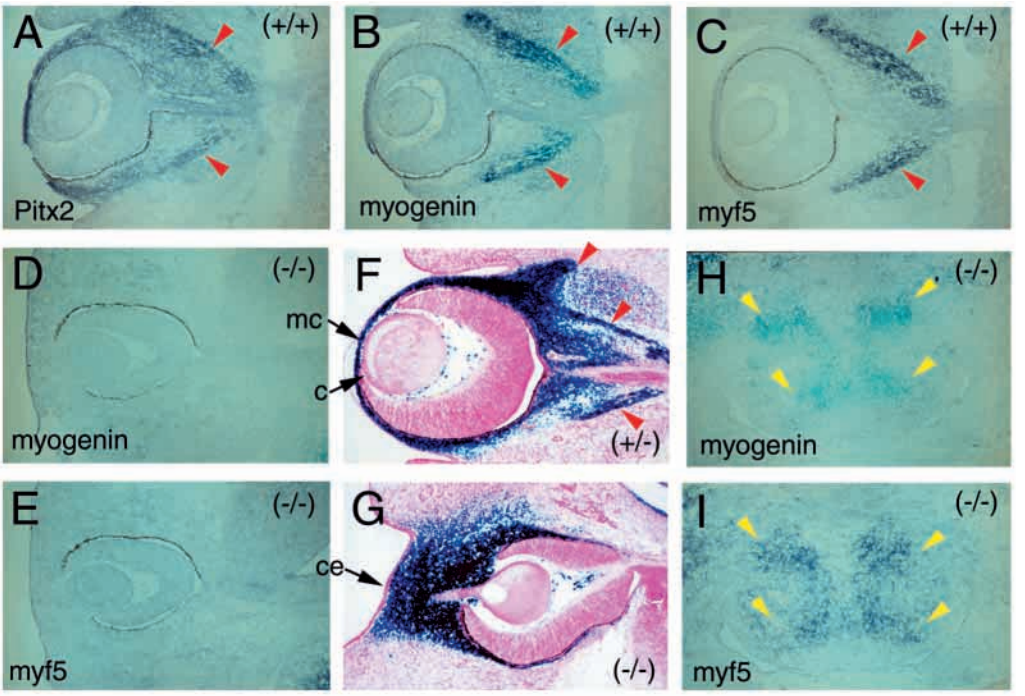

Fig. 7. Extraocular muscle dysgenesis and thickening of the mesothelial layer of the cornea in *Pitx2*$^{-/-}$ embryo. (A-E) In situ hybridization images of Pitx2 (A), myogenin (B,D) and myf5 (C,E) in oculus of *Pitx2*$^{+/+}$ (A-C) and *Pitx2*$^{-/-}$ (D,E) embryos at 12.5 dpc. (A-C) and (D,E) are serial sections, respectively. Colocalization of Pitx2, myogenin and myf5 are seen in the extraocular muscle of a *Pitx2*$^{+/+}$ embryo (red arrowheads). In a *Pitx2*$^{-/-}$ embryo, myogenin and myf5 are not detected in extraocular muscle forming region. (F,G) X-gal-stained images of oculus of *Pitx2*$^{+/-}$ (F) and *Pitx2*$^{-/-}$ (G) embryos at 13.5 dpc. In *Pitx2*$^{+/-}$ oculus, extraocular muscle (red arrowheads) and the mesothelial layer (mc) of the cornea are *lacZ* positive. In *Pitx2*$^{-/-}$ oculus, *lacZ*-positive cells could not be found in the extraocular muscle forming region. On the other hand, the thickening of the *lacZ* positive mesothelial layer of the cornea is seen between cuboidal epithelium making up the anterior part of the lens (c) and cornea ectoderm (ce). Invasion of the cuboidal epithelium of the anterior lens into the thick mesothelial layer of the cornea is observed in the oculus. (H,I) In situ hybridization images of myogenin (H) and myf5 (I) in tongue of *Pitx2*$^{-/-}$ embryos at 12. 5 dpc. (H,I) are serial sections. Myogenin and myf5 were detected in tongue muscle of *Pitx2*$^{-/-}$ embryos (yellow arrowheads).

et al., 1997). The expression of Pitx2 in lung is stage and site specific, and Pitx2 is expressed only in the left lung bud. This suggests the possibility that a property of "left" in the left lung rudiment may be endowed with the repressive regulation of proliferation in the left endoderm by Pitx2 expression, compared with active proliferation in the right endoderm in the absence of Pitx2.

Cardiac looping has been useful as the earliest morphological marker for determining asymmetry in vertebrate embryos. Mice mutant in FGF8 and SIL showed reversed cardiac looping (Meyers and Martin, 1999; Izraeli et al., 1999). On the other hand, deficiencies of Shh, lefty-1, ActRIIB, and Pitx2 in the present study did not result in reversed cardiac looping, although the mice mutant in lefty-1, ActRIIB and Pitx2 showed alteration in the development of the cardiovascular system (Chiang et al., 1996; Oh and Li, 1997; Meno et al., 1998). Thus, it is thought that determination of lung asymmetry and cardiac looping may occur via different gene pathways.

Congenital cardiovascular anomalies and Pitx2

Congenital cardiovascular anomalies are the most common form of human birth defects and are well characterized anatomically and physiologically. However, there is still little information on the genetic basis for most of these anomalies. In this study the *Pitx2*$^{-/-}$ hearts were characterized by a common AV valve with ventricular septal defect and a common atrium showing an ostium primum atrial septal defect. In humans the morphology of the heart in the *Pitx2*$^{-/-}$ embryos is similar with a complete type of AV septal defect (AVSD; Feldt et al., 1995). After cardiac looping, it is generally assumed that the AV canal shifts to the right side and the outflow tract shifts to the left side (Lamers et al., 1992), following which the right and left atria connect to the right and left ventricles, respectively, to establish the four chambered heart. The pulmonary trunk and aorta then connect to the right and left ventricles, respectively, to establish the normal ventriculoarterial connections. Since the AV cushions showed prominent growth in the *Pitx2*$^{-/-}$ hearts, it is speculated that the right-ward shift of the AV canal is inadequate and causes the left sided juxtaposition of the right atrium appendage. The left-ward shift of the outflow tract is not sufficient to form the normal ventriculoarterial connection. During development in the *Pitx2*$^{-/-}$ embryos, the AV canal region in the heart exhibited prominent growth. The myocardium of this region adjacent to the AV cushion tissues showed *lacZ* expression. It is likely that the myocardium in the AV canal region plays an important role in regulating the transformation of endothelial cells into the cushion mesenchyme (Eisenberg and Markwald, 1995). Therefore, it is thought that disruption of *Pitx2* in the myocardium of the region results in hyperplasia of the cushion tissues. *Pitx2*, although it is one of the genes that mediate asymmetry in vertebrates, seems to be an important gene for cardiac morphogenesis. The Pitx2 mouse model will prove valuable for understanding the developmental mechanism of AVSD.

Muscle differentiation and *Pitx2*

Pitx2 and *Pax3* colocalize in trunk myotome, while only *Pitx2* is expressed in the extraocular muscle region (not shown, Tajbakhsh et al., 1997). Muscle differentiation was seen to proceed normally in trunk myotome and tongue of *Pitx2*$^{-/-}$ embryos, while no extraocular muscle was formed. This suggests two possibilities: *Pitx2* is a key upstream regulatory

gene in extraocular muscle differentiation in place of *Pax3*, or there is no redundancy with another related gene for *Pitx2* functions in the extraocular muscle differentiation. In either case, the extraocular muscle-forming cells in *Pitx2*$^{-/-}$ embryos lose the muscle traits and get mixed with *lacZ*(+) *Pitx2*$^{-/-}$ mesoderm in the anterior periocular region. Another quite different possibility is that the progenitor cells of the extraocular muscles, per se, were lost in *Pitx2*$^{-/-}$ embryos, although the origin of the progenitor cells has not yet been precisely identified.

Rieger's syndrome and Pitx2-deficient mice

The human *Pitx2* gene, *RIEG*, which is responsible for Rieger's syndrome, is the human homolog of *Pitx2a* that is expressed symmetrically (Semina et al., 1996). The mutations in Rieger's syndrome include C-terminal truncations and point mutations in the homeobox as well as splice mutations. The mutated genetic structure of Pitx2a in the *Pitx2*$^{-/-}$ embryos was partially similar to that in Rieger's syndrome. Therefore, common defects were found in the *Pitx2*$^{-/-}$ embryos and Rieger's syndrome patients, such as defects in the umbilical cord and peri- and extraocular mesoderm. Enophthalmos in *Pitx2*$^{-/-}$ embryos is seen in Rieger's syndrome. Furthermore, the thickening of the mesothelial layer of the cornea is referred to as the prestage in iris dysplasia, macrocornea, goniodysgenesis and congenital cataract in Rieger's syndrome. Thus, the present *Pitx2*$^{-/-}$ embryos are useful for understanding the developmental mechanisms of Rieger's syndrome. On the other hand, the contribution of the human homolog of Pitx2a to Rieger's syndrome explains the fact that laterality defects have not yet been reported in the syndrome. The interesting cardiac defects in the *Pitx2*$^{-/-}$ embryos suggest that a part of Rieger-associated abnormalities may possibly be caused by a deficiency of human homologs of other Pitx2 isoforms (Kulharya et al., 1995).

The involvement of Pitx2 in craniofacial, tooth, pituitary and heart morphogenesis has been described very recently (Lu et al., 1999; Lin et al., 1999; Gage et al., 1999).

The authors express their appreciation to Dr Austin G. Smith for the ES-cell line E14TG2a, Dr Kazunori Hanaoka for the TK gene cassette, Dr Takashi Takeuchi for the *IRES-T-lacZ* cassette, Dr Naohiro Hashimoto for the *myogenin* and *myoD* clones, Drs Shosei Yoshida and Kohji Uchiyama for the *myf5* clone, Dr Ayumi Miyake for helpful discussions and Mr. Shinichi Kamijo for providing the mouse embryos.

REFERENCES

Bellusci, S., Grindley, J., Emoto, H., Itoh, N. and Hogan, B. L. M. (1997). Fibroblast growth factor 10 (FGF10) and branching morophogenesis in the embryonic mouse lung. *Development* **124**, 4867-4878.

Boer, P. H., Potten, H., Adra, C. N., Jardine, K., Mullhofer, G. and McBurney. M. W. (1990). Polymorphisms in the coding and noncoding regions of murine Pgk-1 alles. *Biochem. Genet.* **28**, 299-308.

Campione, M., Steinbeisser, H., Schweickert, A., Deissler, K., van Bebber, F., Lowe, L. A., Nowotschin, S., Viebahn, C., Haffter, P., Kuehn, M. R. and Blum, M. (1999). The homeobox gene *Pitx2*: mediator of asymmetric left-right signaling in vertebrate heart and gut looping. *Development* **126**, 1225-1234.

Chiang, C., Litingtung, Y., Lee. E., Young, K. E., Corden, J. L., Westphal, H. and Beachy, P. A. (1996). Cyclopia and defective axial patterning in mice lacking Sonic hedgehog gene function. *Nature* **383**, 407-413.

Eisenberg, L. M. and Markwald, R. R. (1995). Molecular regulation of atrioventricular valvuloseptal morphogenesis. *Cir. Res.* **77**,1-6.

Feldt, R. H., Porter, C. J., Edwards, W. D., Puga, F. J. and Seward, J. B. (1995). Atrioventricular septal defects. In *Heart Disease In Infants, Children, and Adolescents* 5th ed (ed. G. C. Emmanouilides et al.), pp. 704-710. Bartimore: Williams & Wilkins.

Gage, P. J. and Camper, S. A. (1997). Pituitary homeobox 2, a novel member of the bicoid-related famoly of homeobox genes, is a potential regulator of anterior structure formation. *Hum. Mol. Genet.* **6**, 457-464.

Gage, P. J., Hookyo, S. and Camper, S. A. (1999). Dosage requirement of Pitx2 for development of multiple organs. *Developmet* **126**, 4643-4651.

Hogan, B., Beddington, R., Costantini, F. and Lacy, E. (1994). Staining embryos for cartilage and bone. In *Manipulating the Mouse Embryo*. pp. 379-380. New York: Cold Spring Harbor Laboratory Press.

Hummel, K. P. and Chapman, D. B. (1959). Visceral inversion and assocoiated anomalies in the mouse. *J. Hered*. **50**, 9-13.

Izraeli, S., Lowe, L. A., Bertness, V. L., Good, D. J., Dorward, D. W., Kirsch, I. R., and Kuehn, M. R. (1999). The SIL gene is required for mouse embryonic axial development and let-right specification. *Nature* **399,** 691-694.

Jorgenson, R. J., Levin, L. S., Cross, H. E., Yoder, F. and Kelly, T. E. (1978). The Rieger syndrome. *Am. J. Med. Gen*. **2**, 307-318.

Kaufman, M. H. (1998). *The Atlas of Mouse Development*. New York: Academic Press.

Kitamura, K., Miura, H., Yanazawa, M., Miyashita, T. and Kato, K. (1997). Expression patterns of Brx1 (Rieg gene), Sonic hedgehog, Nkx2.2, Dlx1 and Arx during zona limitans intrathalamica and embryonic ventral lateral geniculate nuclear foramation. *Mech. Dev.* **67**, 83-96.

Kulharya, A. S., Mabbery, M., Kukolich, M. K., Day, D. W., Schneider, N, R., Wilson, G. N. and Tonk, V. (1995). Interstitial deletions 4q21.1q25 and 4q25q27:phenotypic variability and relation to Rieger anomaly. *Am. J. Med. Genet.* **55**, 165-170.

Lamers, W. H., Wessels, A., Verbeek, F. J., Moorman, A. F. M., Viragh, S., Wenink, A. C. G., Gittenberger-de Groot, A. and Anderson, R. H. (1992). New findings concerning ventricular septation in the human heart. *Circulation* **86**,1194-1205

Lin, C. R., Kioussi, C., O'Connell, S., Briata, P., Szeto, D., Liu, F., Izpisua-Belmonte, J, C. and Rosenfeld, M. G. (1999). Pitx2 regulates lung asymmetry, cardiac positioning and pituitary and tooth morphogenesis. *Nature* **401**, 279-282.

Logan, M., Pagan-Westphal, S. M., Smith, D. M. Paganessi and Tabin, C. J. (1998). The transcription factor Pitx2 mediates situs-specific morphogenensis is response to left-right asymmteric signals. *Cell* **94**, 307-317.

Lu, M-F., Pressman, C., Dyer, R., Johnson, R. L. and Martin, J. F. (1999). Function of Rieger syndrome gene in left-right asymmetry and carniofacial development. *Nature* **401**, 276-278.

Meyers, E. N. and Martin, G. R. (1999). Difference in left-right axis pathways in mouse and chick: functions of FGF8 and Shh. *Scince* **285**, 403-406.

Meno, C., Shimono, A., Saijoh, Y., Yashiro, K., Mochida, K., Ohishi, S., Noji, S., Kondoh, H. and Hamada, H. (1998). lefty-1 is required for left-right determination as a regulator of lefty-2 and nodal. *Cell* **94,** 287-297.

Miller, S. and White, R. D. (1998). Right-left asymmetry of cell proliferation predominates in mouse embryos undergoing clockwise axial rotation. *Anat. Rec.* **250**, 103-108.

Mucchielli, M-L., Marinez, S., Pattyn, A., Goridis, C. and Brunet, J.-F. (1996). Otlx2, an Otx-related homeobox gene expressed in the pituitary gland and in the restricted pattern in the forebrain. *Mol. Cell. Neurosci.* **8**, 258-271.

Oh, S. P. and Li, E. (1997). The signaling pathway mediated by the type IIB activin receptor controls axial patterning and lateral asymmetry in the mouse. *Genes Dev.* **11**, 1812-1826.

Piedra, M. E., Icardo, J. M., Albajar, M., Rodoriguez-Rey, J. C. and Ros, M. A. (1998). Pitx2 participates in the late phase of the pathway controlling left-right asymmetry. *Cell* **94**, 319-324.

Rieger, H. (1935). Dysgenesis mesodemalis corneal et iridis. *Z. Augenheilk* **86**, 333.

Ryan, A. K., Blumberg, B., Rodriguez-Esteban, C., Yonetani-Tamura, S., Tamura, K., Tsukui, T., de la Pena, J., Sabbagh, W., Greenwald, J., Choe, S., Norris, D. P., Robertson, E, J., Evans, R. M., Rosenfeld, M. G. and Belmonte, J. C. I. (1998). Pitx2 determines left-right asymmetry of internal oragans in vertebrates. *Nature* **394**, 545-551.

Semina, E. V., Reiter, R., Leysens, N. J., Alward, W. L. M., Small, K. W., Datson, N. A, Siegel-Batelt, J., Bierke-Nelson, D., Bitoun, P., Zabel, B. U., Carey, J. C. and Murray, J. C. (1996). Cloning and characterization of a novel bicoid-related homeobox transcription factor gene, RIEG, involved in Rieger syndrome. *Nature Genet*. **14**, 392-399.

St. Amand, T, R., Ra, J., Zhang, Y., Hu, Y., Baber,S. I., Qiu, M. and Chen, Y. (1998). Cloning and expression pattern of chicken Pitx2: a new component in the Shh signaling pathway controlling embryonic heat looping. *Biochem. Biophys. Rec. Comm*. **347**, 100-105.

Tajbakhsh, S., Rocancourt, D., Cossu, G. and Buckingham, M. (1997). Refinding the genetic hierarchies controlling skeletal myogenesis: Pax-3 and myf-5 act upstream of myoD. *Cell* **89**, 127-138.

Takeuchi, T., Yamazaki, Y., Katoh-Fukui, Y., Tsuchiya, R., Kondo, S., Motoyama J. and Higashinakagawa T. (1995). Gene trap capture of a novel mouse gene, jumonji, required for neural tube formation. *Genes Dev*. **9**, 1211-1222.

Yoshioka, H., Meno, C., Koshiba, K., Sugihara, M., Itoh, H., Ishimaru, Y., Inoue. T., Ohuchi, H., Semina, E. V., Murray, J. C., Hamada, H. and Noji, S. (1998). Pitx2, a bicoid-type homeobox gene, is involved in a lefty-signaling pathway in determination of left-right asymmetry. *Cell* **94**, 299-305.